Soil-water retention behaviour of fine/coarse soil mixture with varying coarse grain contents and fine soil dry densities

Yu Su, Yu-Jun Cui, Jean-Claude Dupla, Jean Canou

Soil-water retention behaviour of fine/coarse soil mixture with varying coarse grain contents and fine soil dry densities

Yu Su[1,2], Yu-Jun Cui[2], Jean-Claude Dupla[2], Jean Canou[2]

1: School of Civil Engineering and Architecture, Nanchang University, Nanchang 330031, China

2: Laboratoire Navier/CERMES, Ecole des Ponts ParisTech (ENPC), France

Corresponding author

Yu SU

1. School of Civil Engineering and Architecture, Nanchang University, Nanchang 330031, China

2. Ecole des Ponts ParisTech, Laboratoire Navier/CERMES, 6 – 8 av. Blaise Pascal, Cité Descartes, Champs-sur-Marne, 77455 Marne – la – Vallée cedex 2, France

E-mail address: yu.su@enpc.fr

Abstract

An interlayer soil identified in the French conventional rail track corresponded to a mixture of fine soil and coarse grains. To investigate the role of fines in the soil-water retention property of such mixture, different coarse grain contents f_v and dry densities of fine soil $\rho_{d\text{-}f}$ were considered. The filter paper method was applied to measure the matric suction. Mercury intrusion porosimetry tests were performed for the microstructure observation of fine soil. In terms of gravimetric water content of fine soil w_f with matric suction ψ, the soil-water retention curve (SWRC) was significantly affected by $\rho_{d\text{-}f}$ for $\psi < 715$ kPa, while independent of $\rho_{d\text{-}f}$ for $\psi > 715$ kPa. Interestingly, this threshold ψ corresponded to a delimiting pore diameter of bi-modal microstructure of fine soil, which separated micro-pores from macro-pores. In terms of degree of saturation S_r with ψ, the SWRC was significantly affected by $\rho_{d\text{-}f}$ in the full suction range, while independent of f_v. These findings help better understand the results on samples with the dry density of mixture ρ_d kept constant: an increase of f_v resulted in a decrease of $\rho_{d\text{-}f}$ and the suction changed accordingly. In that case, both f_v and ψ affected the mechanical behavior.

Keywords: soil-water retention; matric suction; pore size distribution; dry density; coarse grain content

INTRODUCTION

In the French conventional rail track, an interlayer was naturally created in the substructure under the long-term traffic loading, which corresponded to a mixture of ballast grains and subgrade fine soil. As its suction can greatly affect its mechanical behavior (see details in Su et al. 2020a and Wang et al. 2018), it appears important to investigate its water retention property in-depth.

In-situ investigations showed a decrease of ballast grain content with the increasing depth of interlayer soil (Trinh 2011, Cui et al. 2013). Globally, the interlayer soil was separated into two parts: the upper part was characterized by a coarse grain skeleton fabric, and the lower part by a fine matric macrostructure with dispersed coarse grains. In addition, due to the different vertical stresses over depths, the dry density of fine soil $\rho_{d\text{-}f}$ was different. Wang et al. (2017, 2018), Cui (2018) and Qi et al. (2020a) studied the effect of coarse grain content f_v (the ratio of the volume of coarse grains V_c to the volume of total sample V) on the mechanical behavior of interlayer soil at a constant $\rho_{d\text{-}f}$ = 1.82 Mg/m^3. They assumed that under a given water content, the matric suction of mixture was the same at a constant $\rho_{d\text{-}f}$ = 1.82 Mg/m^3. Up to now, this point has not been experimentally examined yet. It seems necessary to verify this point by investigating the effects of coarse grain content f_v and dry density of fine soil $\rho_{d\text{-}f}$ on the soil-water retention property of fine/coarse soil mixture.

The effects of dry density and coarse grain content on soil-water retention property were investigated previously in some studies. The filter paper method (ASTM D5298-10, 2010) was usually adopted for the measurement of suction (Muñoz-Castelblanco et al. 2010; Kim et al. 2015; Jing 2017). It appeared that the effect of dry density on soil-water retention behavior

was strongly dependent on the microstructure (Simms and Yanful 2002; Romero et al. 2011). Romero et al. (1999) studied the effect of dry density on water retention and microstructure of Boom clay by vapor equilibrium technique and mercury intrusion porosimetry tests, respectively. The results showed that the soil-water retention curve (SWRC) in the low suction range was governed by the inter-aggregate pores, while that in high suction range was governed by intra-aggregate pores. Similarly, Salager et al. (2013) and Gao and Sun (2017) investigated the water retention capacity of clayey soil and found that the SWRCs for different dry densities was independent of dry density beyond a certain matric suction. It is worth noting that these studies only involved the effect of dry density without the effect of coarse grain content. Fiès et al. (2002) studied the soil-water retention property of fine soil/glass fragments mixture, and found that an increasing glass content led to a reduction of the amount of water stored in the mixture. Baetens et al. (2009) investigated the effect of rock fragments on the water retention property of stony soil, and reported that rock fragments could affect the SWRC when the matric suction was smaller than 30 kPa. Duong et al. (2014) studied the hydraulic behavior of interlayer soil by infiltration column, and observed that increasing coarse grain content resulted in a lower SWRC or a lower water retention capacity. Note that in most of these studies, the effect of coarse grain content on soil-water retention property of mixture was investigated with a large quantity of coarse grains, which corresponded to the coarse grain skeleton structure of mixture, without considering the fine matric macrostructure. In addition, the dry density of mixture ρ_d was taken constant, leading to a decrease of dry density of fine soil $\rho_{d\text{-}f}$ with the increase of coarse grain content. That would increase the difficulty of analysis while studying the effect of suction.

This study aims to investigate the effects of coarse grain content f_v and dry density of fine soil $\rho_{d\text{-}f}$ on soil-water retention property of fine/coarse soil mixture. Three f_v = 0%, 20% and 35% were adopted at the same $\rho_{d\text{-}f}$ = 1.82 Mg/m^3 for studying the effect of f_v, and three $\rho_{d\text{-}f}$ =1.82, 1.67 and 1.52 Mg/m^3 were adopted at the same f_v = 0% for studying the effect of $\rho_{d\text{-}f}$. The filter paper method was applied to measure the matric suction of soil mixture. The microstructure of fine soil under varying $\rho_{d\text{-}f}$ values was determined by mercury intrusion porosimetry tests. The results obtained allowed the effects of f_v and $\rho_{d\text{-}f}$ on soil-water retention property of soil mixture to be clarified.

MATERIALS AND METHODS

Fine soil and coarse grains

Considering the difficulty of extracting intact interlayer soil from the field, the reconstituted fine soil and coarse grains were fabricated in the laboratory. For the fine soil fraction, to obtain a similar grain size distribution of fines from 'Senissiat site' (Trinh 2011) (Fig. 1), nine different mass proportions of commercial soils were mixed (Table 1; see details in Lamas-Lopez 2016). The liquid limit and plasticity index of the reconstituted fine soil were 32% and 20%, respectively. Consequently, a good agreement between in-situ fine soil and reconstituted fine soil was observed in terms of grain size distribution, plasticity index and liquid limit (see details in Wang et al. 2017). Fig. 2 presents the standard Proctor compaction curve of the reconstituted fine soil, defining an optimum water content $w_{opt\text{-}f}$ = 13.7% and a maximum dry density $\rho_{dmax\text{-}f}$ = 1.82 Mg/m^3. Note that the $\rho_{dmax\text{-}f}$ = 1.82 Mg/m^3 of reconstituted fine soil was consistent with the $\rho_{d\text{-}f}$ = 1.80 Mg/m^3 of in-situ fine soil measured by Lamas-Lopez (2016).

Based on above features, the reconstituted fine soil was considered as representative of the in-situ fine soil. For the coarse grains fraction, the micro-ballast was adopted to replace the real ballast by following a parallel gradation method adopted by Wang et al. (2017) and Su et al. (2020a). The validity of this method was verified by Qi et al. (2020b), who performed comparisons between micro-ballast and ballast in terms of mechanical behavior under static and cyclic loadings. Note that the scaled fine/coarse soil mixture was used as representative of interlayer soil taken from Senissiat (near Lyon, France, Trinh 2011), which was far from the coastal. Thus, the salt content-related osmotic suction was ignored and only the matric suction was taken into account in this study.

Parameter f_v, widely adopted in previous studies (Seif El Dine et al. 2010; Wang et al. 2017, 2018; Su et al. 2020a, 2020b), was considered in this study. Based on the definition of f_v (Eq.(1)), which only quantified the amount of dry coarse grains in the mixture, all voids and water were assumed to be contained in the fine soil (Fig. 3), as in Wang et al. (2018) and Su et al. (2020a). Based on this assumption, the degree of saturation S_r of mixture can be related to the fine soil fraction. :

$$f_v = \frac{V_c}{V} = \frac{V_c}{V_c+V_f} = \frac{V_c}{V_c+V_{s-f}+V_{w-f}+V_{a-f}} \quad (1)$$

where V_f is the volume of fine soil; $V_{s\text{-}f}$, $V_{w\text{-}f}$ and $V_{a\text{-}f}$ are the volume of fine grains, water and air in the fine soil.

For the soil mixture at varying f_v, $\rho_{d\text{-}f}$ and water content w_f of fine soil, the mass of coarse grains $m_{s\text{-}c}$, fine grains $m_{s\text{-}f}$ and water content of fine soil $m_{w\text{-}f}$ could be determined as follows:

$$m_{s-c} = V_c \cdot G_{s-c} \cdot \rho_w = f_v \cdot V \cdot G_{s-c} \cdot \rho_w \quad (2)$$

$$m_{s-f} = \rho_{d-f} \cdot V_f = \rho_{d-f} \cdot V \cdot (1 - f_v) \quad (3)$$

$$m_{\mathrm{w-f}} = w_{\mathrm{f}} \cdot m_{\mathrm{s-f}} \quad (4)$$

where $G_{\mathrm{s\text{-}c}}$ is the specific gravity of coarse grains; ρ_{w} is the water unit mass.

For the soil mixture at a given $\rho_{\mathrm{d\text{-}f}}$, the corresponding void ratio of fine soil e_{f} could be deduced using Eq. (5):

$$e_{\mathrm{f}} = \frac{G_{\mathrm{s-f}} \cdot \rho_{\mathrm{w}}}{\rho_{\mathrm{d-f}}} - 1 \quad (5)$$

where $G_{\mathrm{s\text{-}f}}$ is the specific gravity of fine soil.

Then, the void ratio e_{m} of soil mixture can be determined:

$$e_{\mathrm{m}} = \frac{V_{\mathrm{v-f}}}{V_{\mathrm{c}} + V_{\mathrm{s-f}}} = \frac{V_{\mathrm{v-f}}}{V - V_{\mathrm{v-f}}} \quad (6)$$

$$V_{\mathrm{v-f}} = e_{\mathrm{f}} \cdot V_{\mathrm{s-f}} \quad (7)$$

$$V_{\mathrm{s-f}} = \frac{m_{\mathrm{s-f}}}{G_{\mathrm{s-f}} \cdot \rho_{\mathrm{w}}} \quad (8)$$

where $V_{\mathrm{v\text{-}f}}$ is the volume of voids in fine soil; $V_{\mathrm{s\text{-}f}}$ is the volume of fine grains.

Combining Eqs. (1), (3) and (5)-(8), the void ratio e_{m} of soil mixture at varying f_{v} and $\rho_{\mathrm{d\text{-}f}}$ was obtained:

$$e_{\mathrm{m}} = -1 + \frac{1}{1 - \frac{(G_{\mathrm{s-f}} \cdot \rho_{\mathrm{w}} - \rho_{\mathrm{d-f}}) \cdot (1 - f_{\mathrm{v}})}{G_{\mathrm{s-f}} \cdot \rho_{\mathrm{w}}}} \quad (9)$$

Fig. 4 shows the variations of e_{f} and e_{m} with f_{v} at a constant $\rho_{\mathrm{d\text{-}f}}$ = 1.82 Mg/m^3. The e_{f} and e_{m} were obtained by substituting $\rho_{\mathrm{d\text{-}f}}$ = 1.82 Mg/m^3 and $G_{\mathrm{s\text{-}f}}$ = 2.68 (Duong et al. 2016) into Eqs. (5) and (9), respectively:

$$e_{\mathrm{f}} = 0.47 \quad (10)$$

$$e_{\mathrm{m}} = -1 + \frac{1}{1 - 0.32 \cdot (1 - f_{\mathrm{v}})} \quad (11)$$

As mentioned before, all voids and water were assumed to be contained in the fine soil. Thus, the S_{r} represented both degree of saturation of soil mixture and that of fine soil:

$$S_{\mathrm{r}} = \frac{V_{\mathrm{w-f}}}{V_{\mathrm{v-f}}} \quad (12)$$

149 *Filter paper method*

150 The filter paper method (ASTM D5298-10, 2010) was used to measure the matric suction.
151 Filter paper measurement was generally performed by putting a piece of filter paper between
152 two soil disks to attain suction equilibrium between filter paper and soil disks (ASTM D5298-
153 10 2010; Muñoz-Castelblanco et al. 2010; Kim et al. 2015; Jing 2017). Considering the
154 maximum diameter d = 20 mm of coarse grains (Fig. 1), the soil disk was prepared at 100 mm
155 diameter and 100 mm height. As for the preparation of soil disks, the fine soil (Fig. 5(a)) was
156 prepared at a molding water content $w_{\text{opt-f}}$ = 13.7%, then stored in a container for at least 24 h,
157 allowing water homogenization. After that, the fine soil was thoroughly mixed with the coarse
158 grains (Fig. 5(a)) with their pre-determined masses at target f_{v} and $\rho_{\text{d-f}}$ values (Table 2). Note
159 that a characteristic coarse grain content $f_{\text{v-cha}} \approx$ 27% identified by Wang et al. (2018)
160 separated the coarse grain skeleton fabric ($f_{\text{v}} > f_{\text{v-cha}}$) and the fine matrix macrostructure ($f_{\text{v}} <$
161 $f_{\text{v-cha}}$) of mixture. Both fabrics were considered in this study with f_{v} ranging from 0% to 35%.
162 The fine/coarse soil mixture were then compacted in four layers, with an equal amount of fine
163 soil and coarse grains for each layer (Fig. 5(b)). Table 2 presents the variations of e_{f}, S_{r} and the
164 dry density of soil mixture ρ_{d} with f_{v} and $\rho_{\text{d-f}}$ at a molding water content of fine $w_{\text{opt-f}}$ = 13.7%.
165 After compaction, the soil disks at different f_{v} and $\rho_{\text{d-f}}$ values were wetted from the molding
166 states to the saturated state. The approach proposed by Su et al. (2020c) was adopted during
167 the wetting process: 10 g water was distributed uniformly on the surface of soil disk by a
168 sprayer each time. The disk was then covered with plastic film for at least 7 h. Fig. 2 shows
169 that the wetting process of soil disk from a molding state to a nearly saturated state induced a
170 slight decrease of $\rho_{\text{d-f}}$ due to the swelling of fine soil, and consequently a slight increase of e_{f}

and slight decrease of ρ_d (Table 2). The measured w_f and the corresponding S_r of soil disks at nearly saturated state were also presented in Table 2.

To obtain the drying soil-water retention curve of soil mixture at a given f_v and $\rho_{d\text{-}f}$, 10 suction measurements were conducted, corresponding to 10 target w_f values. When a soil disk reached a target w_f value, it was covered with plastic film for at least 24 h prior to measuring its matric suction. A set of three filter paper was prepared, with the middle filter paper (diameter d = 80mm) slightly smaller than the two outer filter paper (d = 90mm) to avoid contamination of the middle one. The set of three filter papers was then placed between two soil disks. The whole set was covered with plastic film, and then sealed with wax. Note that an initial water content of 4.61% of the filter paper was measured, corresponding to a suction of 93 MPa. In this case, the filter paper followed a wetting process during the equilibration process between soil and filter paper. After equilibration, the water content of soil disks and the middle filter paper were measured, with a balance of 1/10000 g accuracy. The corresponding matric suction was then determined for varying f_v, $\rho_{d\text{-}f}$ and w_f values. It is worth noting that the volume of soil disks at different w_f values was also measured, by means of a caliper.

Mercury intrusion porosimetry test (MIP)

For the MIP tests, three soil disks were prepared at varying $\rho_{d\text{-}f}$ = 1.82, 1.67 and 1.52 Mg/m^3 with the same f_v = 0%. The freeze-drying method was adopted: fine soil was cut into small pieces of around 1.5 g each, and then immersed into nitrogen under vacuum; afterwards, the frozen soil was transferred to the chamber of a freeze dryer for lyophilizing. This method

193 minimized the microstructure disturbance of fine soil, which was widely used in previous
194 studies (Cui et al. 2002; Delage et al. 2006; Wang et al. 2014).
195
196 RESULTS
197 To determine the equilibration time of samples with the filter paper method, three samples
198 were prepared at the same f_v = 0%, $\rho_{d\text{-}f}$ = 1.82 Mg/m^3 and $w_{opt\text{-}f}$ = 13.7%, with 5, 7 and 9 days
199 waited, respectively. Fig. 6 depicts the variations of matric suction and water content of filter
200 paper with time. It appears that with the increase of time from 0 to 5, 7 and 9 days, the water
201 content of filter paper increased from 4.61% to 30.59%, 32.02% and 32.11%, and the
202 corresponding matric suction decreased from 93 MPa to 879, 679 and 670 kPa, respectively.
203 This indicated that at least a time of 7 days was needed for the suction equilibration between
204 soil and filter paper. Thereby, a duration of 7 days was adopted for all tests.
205 Fig. 7 shows the drying SWRC expressed in terms of w_f and S_r with ψ and the variations
206 of e_f with ψ for different f_v values (0%, 20% and 35%) and different initial $\rho_{d\text{-}f}$ values (1.82,
207 1.67 and 1.52 Mg/m^3). The retention curves were fitted with the van Genuchten model (1980).
208 The legends were defined following the rule: 'f_v 0%- $\rho_{d\text{-}f}$1.82' refers to the f_v = 0% and the
209 initial $\rho_{d\text{-}f}$ = 1.82 Mg/m^3. Fig. 7(a) depicts the variations of w_f with ψ for various f_v and $\rho_{d\text{-}f}$
210 values. It appears clearly that the water retention curves were only dependent on the dry
211 density of fines $\rho_{d\text{-}f}$, and independent of the coarse grain content f_v. In addition, the gaps
212 between the three curves for different $\rho_{d\text{-}f}$ values decreased with the increase of matric suction
213 ψ. The curves converged to the same one beyond a threshold suction ψ = 715 kPa. Thus, the
214 SWRC in low suction range (ψ < 715 kPa) was sensitive to the variation of $\rho_{d\text{-}f}$, while

215 independent of $\rho_{d\text{-}f}$ in high suction range (ψ > 715 kPa).

216 Fig. 7(b) depicts the variations of void ratio of fine soil e_f with ψ for the fine/coarse soil
217 mixture at varying f_v and $\rho_{d\text{-}f}$ values. It appears that such variations were also only dependent
218 on $\rho_{d\text{-}f}$ and independent of f_v. In addition, the lower the $\rho_{d\text{-}f}$ value, the larger the decrease of e_f
219 with increasing ψ, showing a larger volume change under the effect of suction for the case of
220 lower $\rho_{d\text{-}f}$.

221 Fig.7(c) presents the variations of degree of saturation S_r with ψ for the fine/coarse soil
222 mixture at varying f_v and $\rho_{d\text{-}f}$ values. The curves were found to be independent of f_v, which
223 agreed with those in Fig.7 (a)-(b). In addition, the larger the $\rho_{d\text{-}f}$ value the higher the water
224 retention capacity. With the decrease of $\rho_{d\text{-}f}$ from 1.82 to 1.67 and 1.52 Mg/m^3, the air entry
225 value (AEV) decreased from 550 to 96 and 36 kPa respectively.

226 Fig. 8 shows the pore size distributions (PSD) of fine soil at $\rho_{d\text{-}f}$ = 1.82, 1.67 and 1.52
227 Mg/m^3. It can be observed from Fig. 8(a) that a decrease of $\rho_{d\text{-}f}$ resulted in an increase of
228 intruded mercury void ratio e_M, which was a little smaller than the corresponding global e_f.
229 Fig. 8(b) presents typical bi-modal porosity of fine soil, with a delimiting diameter d = 0.65
230 μm for micro- and macro-pores. For compacted soils, the micro-pores were generally within
231 aggregates (intra-aggregate pores), while the macro-pores were between aggregates (inter-
232 aggregate pores) (Delage et al. 1996). With the increase of $\rho_{d\text{-}f}$, the volume of inter-aggregate
233 pores was observed to decrease, while that of intra-aggregate pores was almost constant,
234 suggesting that the compaction process only affected the macro-pores, in agreement with
235 Wang et al. (2014).

236

237 DISCUSSIONS

238 *Effect of microstructure of fine soil on SWRC at varying $\rho_{d\text{-}f}$*

239 Fig. 7(a) shows that $\rho_{\text{d-f}}$ affected the SWRC only for ψ < 715 kPa. Correspondingly, Fig. 8(b)
240 indicates that a decrease of $\rho_{\text{d-f}}$ led to an increase of the volume of inter-aggregate pores (d >
241 0.65 μm) without modifying the volume of intra-aggregate pores (d < 0.65 μm). The
242 delimiting d = 0.65 μm could be associated with an equivalent matric suction based on
243 Laplace's law under the assumption of cylindrical pore shape:

244 $$\Psi = \frac{4T_s \cdot \cos\theta}{d} \quad (13)$$

245 where T_s is the surface tension of water, equal to 0.073 N/m at temperature of 20 ℃; θ is the
246 contact angle between the liquid-air interface and the solid, taken equal to 0° in this study.

247 Substituting d = 0.65 μm into Eq. (13), the corresponding ψ was obtained:

248 $$\psi = 449 \text{ kPa} \quad (14)$$

249 It was found that this value was close to the AEV of 550 kPa for the mixture at $\rho_{\text{d-f}}$ = 1.82
250 Mg/m^3 (Fig. 7(c)), which was consistent with the findings of Zhang et al. (2018). This value
251 was smaller than the threshold ψ = 715 kPa in Fig. 7(a). This difference could be explained as
252 follows: the fine soil with varying $\rho_{\text{d-f}}$ values for MIP tests was compacted at a molding water
253 content $w_{\text{opt-f}}$ = 13.7%, while the fine soil corresponding to the threshold point in Fig. 7(a) was
254 subjected to a saturation process from the molding water content $w_{\text{opt-f}}$ = 13.7%, followed by a
255 drying process. Li and Zhang (2009) studied the effect of wetting-drying history on bi-modal
256 porosity of soil, and found that the drying process induced shrinkage of soil, leading to
257 smaller intra-aggregate pores. Similarly, Sun and Cui (2020) investigated the soil-water
258 retention curve of reconstituted silt, and reported that the drying process led to a shrinkage of

soil and a smaller value of diameter of voids. It could be thus inferred that the larger threshold ψ = 715 kPa in Fig. 7(a) was the consequence of pore size decrease due to soil shrinkage shown in Fig. 8(b). It could be thus deduced that in low suction range (ψ < 715 kPa) the SWRC was governed by inter-aggregate pores, while in high suction range (ψ > 715 kPa) the SWRC was governed by intra-aggregate pores. The similar phenomenon was reported by Salager et al. (2013) while studying the water retention property of clayey soil. They identified a threshold suction ψ = 5000 kPa separating the inter-aggregate governing suction from intra-aggregate governing suction. With the decrease of $\rho_{d\text{-}f}$, the volume of inter-aggregate pores increased (Fig. 8(b)), resulting in an increase of water volume in inter-aggregate pores; thereby, an increase of w_f was observed (Fig. 7(a)). However, such decrease of $\rho_{d\text{-}f}$ did not affect the volume of intra-aggregate pores (Fig. 8(b)); thus, a constant w_f was observed in high suction range (Fig. 7(a)). This also confirmed that the compaction effort greatly affected the inter-aggregate pores without touching the intra-aggregate pores (Delage et al. 1996).

Two categories of fine soil in the mixture at f_v = 35% were reported by Su et al. (2020c, 2021): a relatively dense fine soil in between coarse grains and a relatively loose fine soil in macro-pores among coarse grains. In other words, while compacted to $\rho_{d\text{-}f}$ =1.82 Mg/m^3, the dense fines had a higher $\rho_{d\text{-}f}$ and the loose fines had a lower $\rho_{d\text{-}f}$, with the global $\rho_{d\text{-}f}$ being 1.82 Mg/m^3. Thereby, a higher SWRC was expected for the dense fine soil in between coarse grains and a lower SWRC for the loose fine soil in macro-pores among coarse grains. However, as the SWRC at f_v = 35% was the same as that at f_v = 0% and 20% for $\rho_{d\text{-}f}$ = 1.82 Mg/m^3 (Fig. 7(c)), it could be inferred that in spite of the inhomogeneous distribution of fine

281 soil in the mixture, the SWRC appeared to be controlled by the global dry density of fine soil
282 $\rho_{d\text{-}f}$ only. Similarly, Zeng et al. (2020) studied the axial swelling property of compacted
283 bentonite/claystone mixture, and found that this behavior was mainly dependent on the global
284 ρ_d of mixture, irrespective of its heterogeneity.
285
286 *Comparison of present study at constant $\rho_{d\text{-}f}$ with previous study at constant ρ_d*
287 In present study, the different f_v = 0%, 20% and 35% corresponded to the same SWRC under
288 the constant $\rho_{d\text{-}f}$ = 1.82 Mg/m^3 (Fig. 7(c)). On the contrary, Duong et al. (2014) investigated
289 the hydraulic behavior of the upper part interlayer soil with two different f_v = 50.3% and
290 55.5% and a constant dry density of mixture ρ_d = 2.01 Mg/m^3 by infiltration column (Table 3).
291 Fig. 9 shows that an increase of f_v from 50.3% to 55.5% led to a lower SWRC under the
292 constant ρ_d = 2.01 Mg/m^3. This phenomenon could be attributed to the effect of $\rho_{d\text{-}f}$ on SWRC.
293 Fig. 10 shows a constant e_m = 0.33 (corresponding to ρ_d = 2.01 Mg/m^3) for f_v = 50.3% and
294 55.5% in Duong et al. (2014), which was different from that in Fig. 4 of present study. While
295 increasing f_v from 50.3% to 55.5%, the e_f was increased from 1.01 to 1.28; thereby, a decrease
296 of $\rho_{d\text{-}f}$ from 1.33 to 1.17 Mg/m^3 (Table 3). As a result, the increase of f_v from 50.3% to 55.5%
297 led to a lower SWRC (Fig. 9).
298
299 *The maximum degrees of saturation S_r of samples*
300 It appears from Fig. 7(c) and Fig. 9 that the SWRCs all started at a degree of saturation S_r
301 lower than 100%. Moreover, the values in Fig. 9 (S_r = 91% and 78% for f_v = 50.3% and 55.5%
302 respectively) were smaller than the values around S_r = 95% for varying f_v = 0%, 20% and 35%

303 at $\rho_{d\text{-}f}$ = 1.82 Mg/m^3 in Fig. 7(c), showing that the maximum S_r value reached during the
304 saturation process decreased with the increase of f_v. Saba et al. (2014) worked on a
305 compacted sand/bentonite mixture and found that the fine grains of larger sizes (e.g. the
306 maximum d = 2 mm) was preferentially arranged with a large face side in the horizontal
307 direction. In addition, due to the restriction of mould wall, more macro-pores were formed in
308 the side part of sample, as evidenced by Zeng et al. (2020) on a compacted
309 bentonite/claystone mixture. Such preferential presence of macro-pores in the side part was
310 further confirmed on the mixture of fine soil and micro-ballast by Wang et al. (2018) and Qi et
311 al. (2020a) through observation at X-ray μCT. As these macro-pores could not retain water
312 under the effect of gravity, a maximum value of S_r = 95% was obtained. With the increase of f_v,
313 the addition of coarse grains increased the mould wall restriction effect, generating thus more
314 macro-pores. This led to a decrease of the initial S_r value of the SWRC with f_v. It is worth
315 noting that Duong et al. (2014) adopted the ballast grains of maximum d = 60 mm to prepare
316 the sample of d = 300 mm and h = 600 mm, while in this study the micro-ballast of maximum
317 d = 20 mm (Fig. 1) was adopted to prepare soil disk of d = 100 mm and h = 100 mm. Much
318 larger mould wall restriction effect was thus expected in the case of Duong et al. (2014) due to
319 the larger dimensions of the grains and the sample. Consequently, much lower maximum
320 degrees of saturation (S_r = 91% and 78% for f_v = 50.3% and 55.5%) were obtained in their
321 case.
322
323 CONCLUSIONS
324 To investigate the role of fine soil on the soil-water retention property of fine/coarse soil

mixture, three f_v = 0%, 20% and 35% at the same $\rho_{d\text{-}f}$ = 1.82 Mg/m^3 and three $\rho_{d\text{-}f}$ = 1.82, 1.67 and 1.52 Mg/m^3 at the same f_v = 0% were considered. A filter paper method was applied to measure the matric suction of soil mixture at different water contents. Mercury intrusion porosimetry tests were performed for microstructure observation of fine soil at varying $\rho_{d\text{-}f}$. The results obtained allowed the following conclusions to be drawn.

The drying SWRC of mixture was found to be only dependent on $\rho_{d\text{-}f}$ and independent of f_v. A typical bi-modal microstructure of fine soil was identified for varying $\rho_{d\text{-}f}$ values, defining a micro-pore and a macro-pore populations. When expressed in terms of w_f with ψ, the SWRC was found to be significantly affected by $\rho_{d\text{-}f}$ for the matric suction ψ lower than 715 kPa. By contrast, when ψ was higher than 715 kPa, the SWRC kept the same, independent of $\rho_{d\text{-}f}$. Interestingly, a delimiting pore diameter d = 0.65 µm was identified, separating micro-pores (or intra-aggregate pores) from macro-pores (or inter-aggregate pores). This delimiting diameter corresponded to a matric suction of 449 kPa, which was smaller than the threshold ψ = 715 kPa due to the effect of volume change experienced in the course of soil wetting/drying from the remolded state ($w_{opt\text{-}f}$ = 13.7%). Thus, the SWRC in low suction range (ψ < 715 kPa) was governed by macro-pores, while in high suction range (ψ > 715 kPa) by micro-pores. In addition, the SWRC of mixture appeared to be controlled by the global fine soil dry density $\rho_{d\text{-}f}$ only. The effect of the possible heterogeneity of fine soil distribution inside the mixture seemed to be negligible.

When expressed in terms of S_r with ψ, the SWRC appeared to be significantly affected by $\rho_{d\text{-}f}$, while unaffected by f_v. This helped better understand the observation of Duong et al. (2014) – the water retention capacity was decreased by the increase of f_v: in the study of

Duong et al. (2014), a constant ρ_d = 2.01 Mg/m^3 was adopted instead of a constant $\rho_{d\text{-}f}$. In this case, an increase of f_v resulted in a decrease of $\rho_{d\text{-}f}$, thereby a decrease of water retention capacity.

The initial S_r of the SWRC appeared to decrease with the increase of f_v. At f_v = 0%, due to the effect of mould wall restriction, macro-pores were formed in the side part of sample. As these macro-pores could not retain water under the effect of gravity, the maximum value of S_r = 95% smaller than 100% was obtained in the saturation process. With the increase of f_v, the addition of coarse grains increased the mould wall restriction effect, generating more macro-pores and thus lower maximum S_r. This phenomenon was expected to be more pronounced in the case of larger grains and larger sample dimensions.

From a practical point of view, these findings suggest that when investigating the water-retention property of interlayer soil, the scaled coarse grains at small size can be used as a substitute for real ballast grains at large size. With the increasing depth of interlayer soil, the decrease of f_v induced no changes on water-retention capacity of interlayer soil, provided that the $\rho_{d\text{-}f}$ of fine soil kept constant. When the water retention property is determined, it can be incorporated in the mechanical models to better describe the variation of permanent strain of unsaturated interlayer soil under the effect of cyclic loadings. In addition, it is worth noting that to some extent these findings can be helpful in evaluating the effects of $\rho_{d\text{-}f}$ and f_v on the water retention property of mixtures with varying types of coarse and fine soil.

ACKNOWLEDGEMENTS

368 This work was supported by the China Scholarship Council (CSC) and Ecole des Ponts
369 ParisTech.

370

371

372 NOTATIONS

e	void ratio
e_f	void ratio of fine soil
e_m	void ratio of fine/coarse soil mixture
f_v	coarse grain content
$f_{v\text{-}cha}$	characteristic coarse grain content
$G_{s\text{-}c}$	specific gravity of coarse grains
$m_{a\text{-}f}$	mass of air in fine soil
$m_{w\text{-}f}$	mass of water in fine soil
$m_{s\text{-}f}$	mass of fine grains
$m_{s\text{-}c}$	mass of coarse grains
ρ_d	dry density of sample
$\rho_{d\text{-}f}$	dry density of fine soil
$\rho_{dmax\text{-}f}$	maximum dry density of fine soil
ρ_w	water unit mass
S_r	degree of saturation
V	volume of fine/coarse soil mixture
V_f	volume of fine soil
$V_{v\text{-}f}$	volume of voids in fine soil
$V_{a\text{-}f}$	volume of air in fine soil
$V_{w\text{-}f}$	volume of water in fine soil
$V_{s\text{-}f}$	volume of fine grains
V_c	volume of coarse grains
$w_{opt\text{-}f}$	optimum water content of fine soil

w_f water content of fine soil

ψ matric suction

373

374

375 REFERENCES

376 ASTM D5298-10. 2010. Standard test method for measurement of soil potential (suction)
377 using filter paper. West Conshohocken, PA: ASTM International.

378 Baetens, J. M., Verbist, K., Cornelis, W. M., Gabriels, D., and Soto, G. 2009. On the
379 influence of coarse fragments on soil water retention. Water resources research, 45(7).

380 Cui, Y.J., Loiseau, C. and Delage, P. 2002. Microstructure changes of a confined swelling soil
381 due to suction. In *Unsaturated Soils: Proceedings of the Third International Conference*
382 *on Unsaturated Soils, UNSAT 2002, 10-13 March 2002, Recife, Brazil* (Vol. 2, p. 593).
383 CRC Press.

384 Cui, Y.J., Duong, T.V., Tang, A.M., Dupla, J.C., Calon, N. and Robinet, A. 2013.
385 Investigation of the hydro-mechanical behaviour of fouled ballast. Journal of Zhejiang
386 University Science A, 14(4), pp.244-255.

387 Cui, Y. J. 2018. Mechanical behaviour of coarse grains/fines mixture under monotonic and
388 cyclic loadings. Transportation Geotechnics, 17, 91-97.

389 Delage, P., Audiguier, M., Cui, Y.J. and Howat, M.D. 1996. Microstructure of a compacted
390 silt. *Canadian Geotechnical Journal*, *33*(1), pp.150-158.

391 Delage, P., Marcial, D., Cui, Y.J. and Ruiz, X. 2006. Ageing effects in a compacted bentonite:
392 a microstructure approach. *Géotechnique*, *56*(5), pp.291-304.

393 Duong, T. V., Cui, Y. J., Tang, A. M., Dupla, J. C., and Calon, N. 2014. Effect of fine
394 particles on the hydraulic behavior of interlayer soil in railway substructure. Canadian
395 geotechnical journal, 51(7), 735-746.

396 Duong, T. V., Cui, Y. J., Tang, A. M., Dupla, J. C., Canou, J., Calon, N., and Robinet, A.
397 2016. Effects of water and fines contents on the resilient modulus of the interlayer soil of
398 railway substructure. Acta Geotechnica, 11(1), 51-59.

399 Fiès, J. C., Louvigny, N. D. E., and Chanzy, A. 2002. The role of stones in soil water retention.
400 European Journal of Soil Science, 53(1), 95-104.

401 Gao, Y., Sun, D. 2017. Soil-water retention behavior of compacted soil with different
402 densities over a wide suction range and its prediction. Computers and Geotechnics,
403 91(nov.):17-26.

404 Jing, P. 2017. Experimental study and modelling of the elastoplastic behaviour of unbound
405 granular materials under large number of cyclic loadings at various initial hydric states
406 (Doctoral dissertation, Université de Strasbourg).

407 Kim, H., Ganju, E., Tang, D., Prezzi, M., and Salgado, R. 2015. Matric suction measurements
408 of compacted subgrade soils. Road Materials and Pavement Design, 16(2), 358-378.

409 Li, X., and Zhang, L. M. 2009. Characterization of dual-structure pore-size distribution of soil.
410 Canadian geotechnical journal, 46(2), 129-141.

411 Lamas-lopez, F. 2016. Field and laboratory investigation on the dynamic behavior of
412 conventional railway track-bed materials in the context of traffic upgrade. PhD Thesis,
413 Ecole Nationale des Ponts et Chaussées, Université Paris-Est.

414 Muñoz-Castelblanco, J. A., Pereira, J. M., Delage, P., and Cui, Y. J. 2010. Suction
415 measurements on a natural unsaturated soil: A reappraisal of the filter paper method. In
416 Unsaturated Soils-Proc. Fifth Int. Conf. on Unsaturated Soils (Vol. 1, pp. 707-712). CRC
417 Press.

418 Qi, S., Cui, Y.J., Chen, R.P., Wang, H.L., Lamas-Lopez, F., Aimedieu, P., Dupla, J.C., Canou,
419 J. and Saussine, G. 2020a. Influence of grain size distribution of inclusions on the
420 mechanical behaviours of track-bed materials. Géotechnique, 70(3), pp.238-247.

421 Qi, S., Cui, Y.J., Dupla, J.C., Chen, R.P., Wang, H.L., Su, Y., Lamas-Lopez, F. and Canou, J.
422 2020b. Investigation of the parallel gradation method based on the response of track-bed
423 materials under cyclic loadings. Transportation Geotechnics, p.100360.

424 Romero, E., Gens, A., and Lloret, A. 1999. Water permeability, water retention and
425 microstructure of unsaturated compacted Boom clay. Engineering Geology, 54(1-2), 117-
426 127.

427 Romero, E., DELLA VECCHIA, G. A. B. R. I. E. L. E., and Jommi, C. 2011. An insight into
428 the water retention properties of compacted clayey soils. Géotechnique, 61(4), 313-328.

429 Simms, P. H., and Yanful, E. K. 2002. Predicting soil—Water characteristic curves of
430 compacted plastic soils from measured pore-size distributions. Géotechnique, 52(4), 269-
431 278.

432 Seif El Dine, B., Dupla, J. C., Frank, R., Canou, J., and Kazan, Y. 2010. Mechanical
433 characterization of matrix coarse-grained soils with a large-sized triaxial device.
434 Canadian Geotechnical Journal, 47(4), 425-438.

435 Salager, S., Nuth, M., Ferrari, A., and Laloui, L. 2013. Investigation into water retention
436 behaviour of deformable soils. Canadian Geotechnical Journal, 50(2), 200-208.

437 Saba, S., Barnichon, J.D., Cui, Y.J., Tang, A.M., Delage, P. 2014. Microstructure and
438 anisotropic swelling behaviour of compacted bentonite/sand mixture. Journal of Rock
439 Mechanics and Geotechnical Engineering 6(2), 126-132.

440 Su, Y., Cui, Y. J., Dupla, J. C., and Canou, J. 2020a. Investigation of the effect of water
441 content on the mechanical behavior of track-bed materials under various coarse grain
442 contents. Construction and Building Materials, 263, 120206.

443 Su, Y., Cui, Y. J., Dupla, J. C., Canou, J., and Qi, S. 2020b. A fatigue model for track-bed
444 materials with consideration of the effect of coarse grain content. Transportation
445 Geotechnics, 100353.

446 Su, Y., Cui, Y.J., Dupla, J.C., Canou, J., Qi, S. 2020c. Developing a sample preparation
447 approach to study the mechanical behavior of unsaturated fine/coarse soil mixture.
448 Geotechnical Testing Journal. https://doi.org/10.1520/GTJ20190450

449 Su, Y., Cui, Y. J., Dupla, J. C., and Canou, J. 2021. Effect of water content on resilient
450 modulus and damping ratio of fine/coarse soil mixture with varying coarse grain contents.
451 Transportation Geotechnics, 100452.

452 Sun, W. J., and Cui, Y. J. 2020. Determining the soil-water retention curve using mercury
453 intrusion porosimetry test in consideration of soil volume change. Journal of Rock
454 Mechanics and Geotechnical Engineering, 12(5), 1070-1079.

455 Trinh, V. N. 2011. Comportement hydromécanique des matériaux constitutifs de plateformes
456 ferroviaires anciennes. PhD Thesis, Ecole Nationale des Ponts et Chaussées, Université
457 Paris-Est.

458 van Genuchten, M. T. 1980. A closed‐form equation for predicting the hydraulic conductivity
459 of unsaturated soils. Soil science society of America journal, 44(5), 892-898.

460 Wang, Q., Cui, Y. J., Tang, A. M., Xiang-Ling, L., and Wei-Min, Y. 2014. Time-and density-
461 dependent microstructure features of compacted bentonite. Soils and Foundations, 54(4),
462 657-666.

463 Wang, H. L., Cui, Y. J., Lamas-Lopez, F., Dupla, J. C., Canou, J., Calon, N., ... and Chen, R.
464 P. 2017. Effects of inclusion contents on resilient modulus and damping ratio of
465 unsaturated track-bed materials. Canadian Geotechnical Journal, 54(12), 1672-1681.

466 Wang, H.L., Cui, Y.J., Lamas-Lopez, F., Calon, N., Saussine, G., Dupla, J.C., Canou, J.,
467 Aimedieu, P. and Chen, R.P. 2018. Investigation on the mechanical behavior of track-bed

materials at various contents of coarse grains. *Construction and Building Materials*, *164*, pp.228-237.

Zhang, F., Cui, Y. J., and Ye, W. M. 2018. Distinguishing macro-and micro-pores for materials with different pore populations. Géotechnique Letters, 8(2), 102-110.

Zeng, Z., Cui, Y. J., Conil, N., and Talandier, J. 2020. Experimental study on the aeolotropic swelling behaviour of compacted bentonite/claystone mixture with axial/radial technological voids. Engineering Geology, 278, 105846.

477

478 LIST OF TABLES

479

LIST OF FIGURES

480

481

Table 1. Constitution of fine soil

Soil classification	Commercial Soil	Mass proportion (%)	Range of grain size (mm)
Sand	C4	16.7	0.0009 – 0.50
	C10	20	0.0009 – 0.25
	HN34	3.3	0.063 - 0.50
	HN31	3.3	0.16 - 0.63
	HN0.4-0.8	6.7	0.25 - 1
	HN0.6-1.6	6.7	0.32 - 2
	HN1-2.5	13.3	0.32 – 3.20
Clay	Speswhite	23.3	0.0003 – 0.01
	Bentonite	6.7	0.001 – 0.01

501

502 Table 2. As-compacted and saturated states of fine/coarse soil mixture

f_v (%)	As-compacted state					Saturated state				
	$\rho_{d\text{-}f}$ (Mg/m^3)	e_f	$w_{opt\text{-}f}$ (%)	S_r (%)	ρ_d (Mg/m^3)	$\rho_{d\text{-}f}$ (Mg/m^3)	e_f	Measured w_f(%)	Measured S_r(%)	ρ_d (Mg/m^3)
	1.82	0.47		78	1.82	1.81	0.48	17.2	95	1.81
0	1.67	0.60		61	1.67	1.65	0.62	22.0	95	1.65
	1.52	0.76	13.7	48	1.52	1.50	0.78	27.3	93	1.50
20	1.82	0.47		78	1.99	1.80	0.49	17.3	95	1.97
35	1.82	0.47		78	2.12	1.80	0.48	17.2	95	2.10

503

Note: f_v represents the volumetric ratio of coarse grains to the fine/coarse soil mixture. $\rho_{d\text{-}f}$, e_f, $w_{f,}$ and $w_{opt\text{-}f}$ represent the dry density, void ratio, water content and optimum water content of fine soil, respectively. S_r represents the degree of saturation of fine soil, which is also the degree of saturation of the mixture. ρ_d represents the dry density of soil mixture.

504

505

506

507 Table 3. Soil properties of Duong et al. (2014)

f_v (%)	ρ_d (Mg/m^3)	e_m	$\rho_{d\text{-}f}$ (Mg/m^3)	e_f
50.3	2.01	0.33	1.33	1.01
55.5			1.17	1.28

508

509 Note: e_m represents the void ratio of soil mixture.

510

511

512

513

514

515

516

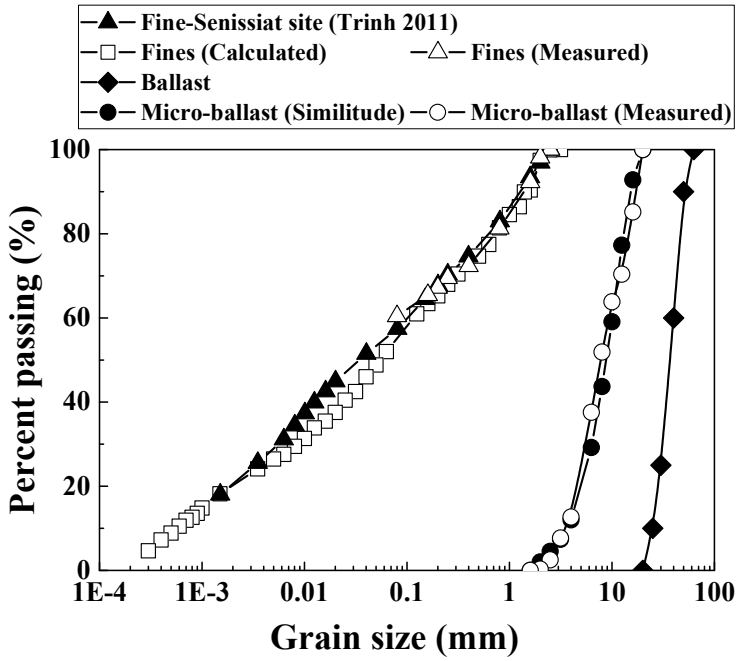

Fig. 1. Grain size distribution curves of fine soil and micro-ballast (after Wang et al. 2017)

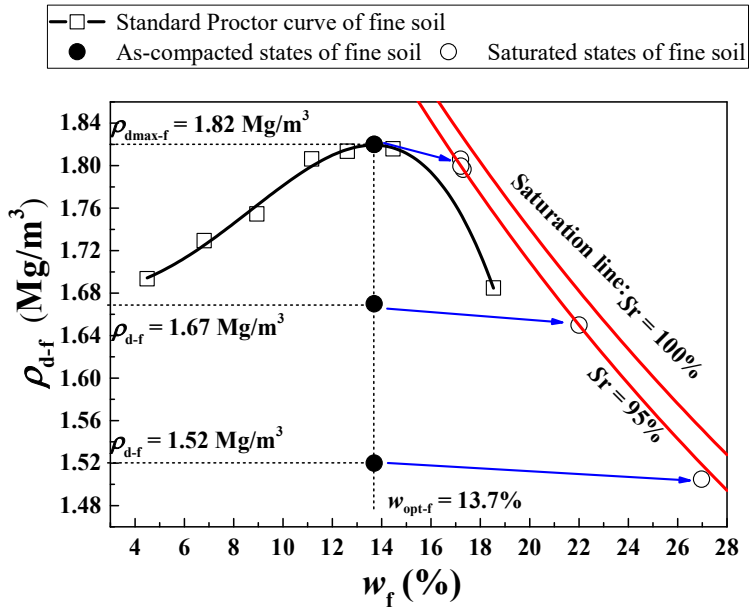

Fig. 2. As-compacted and saturated states of fine soil with respect to its standard Proctor compaction curve

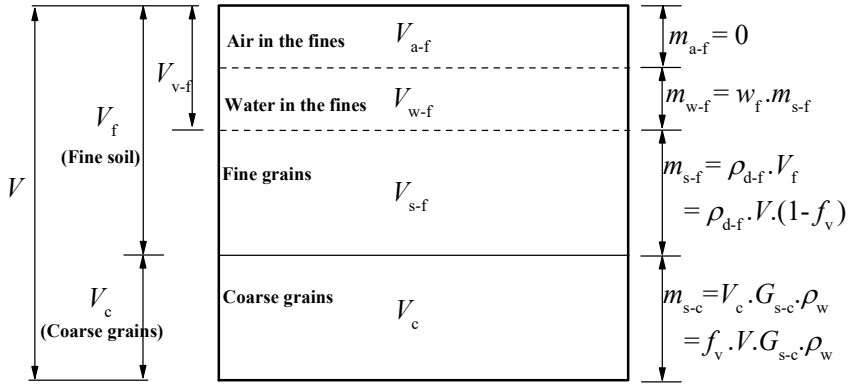

Fig. 3. Constitution of fine/coarse soil mixture

572

573

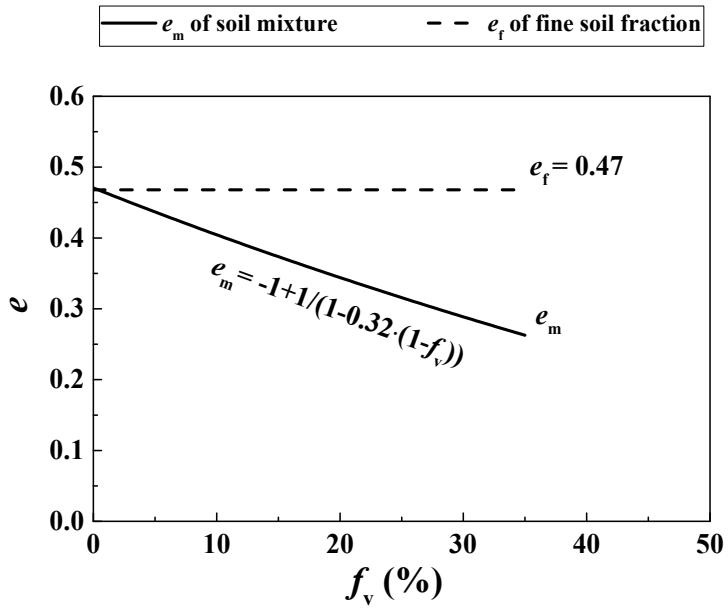

574

575

576 Fig. 4. Variations of void ratios with f_v at a constant $\rho_{d\text{-}f}$ = 1.82 Mg/m^3

577

578

579

580

581

582

583

584

585

586

587

588

589

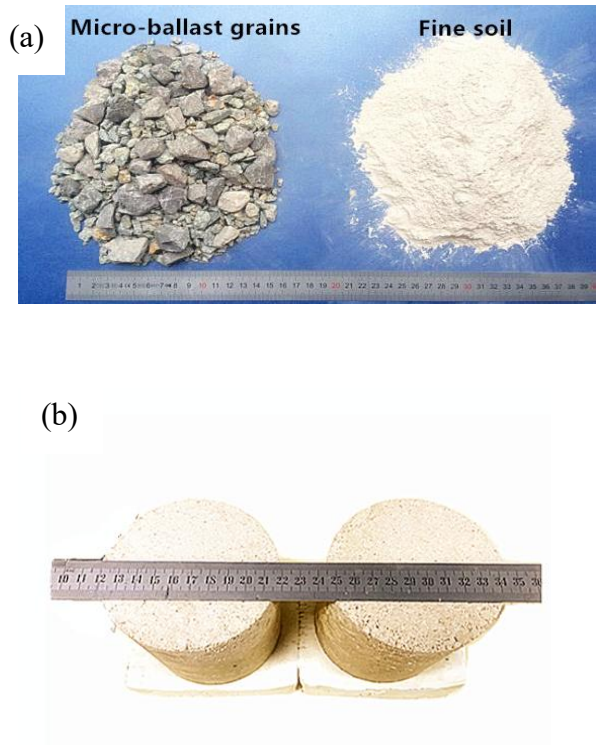

Fig. 5. (a) Preparation of fine soil and micro-ballast and (b) compaction of two soil disks

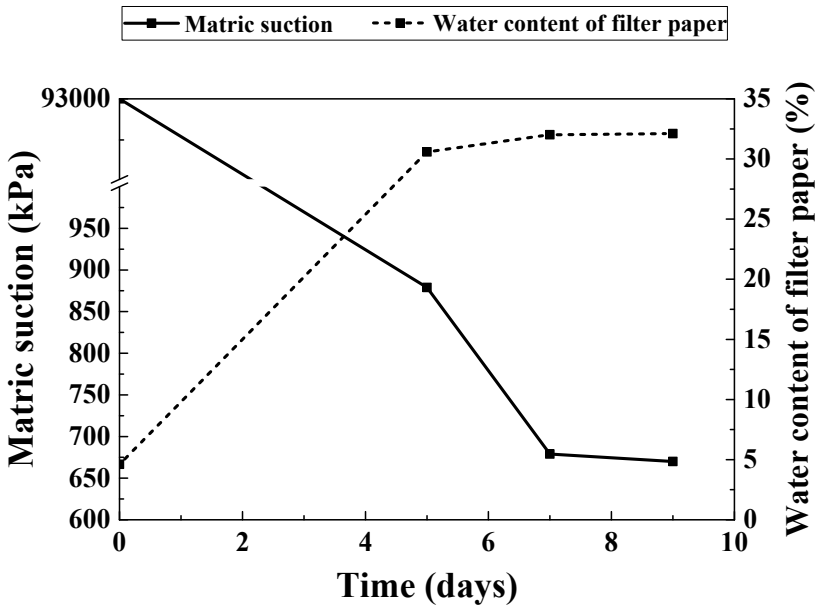

Fig. 6. Determination of equilibration time by filter paper method

634

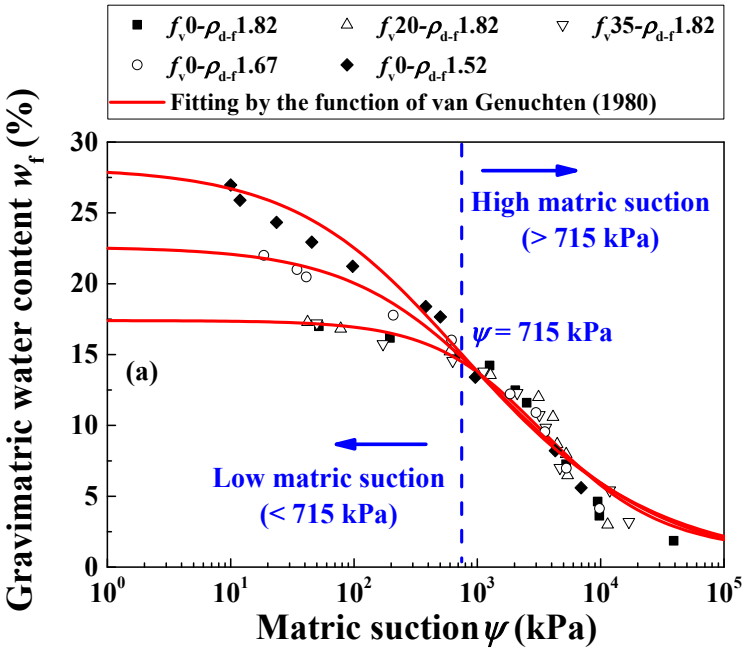

635

636

637

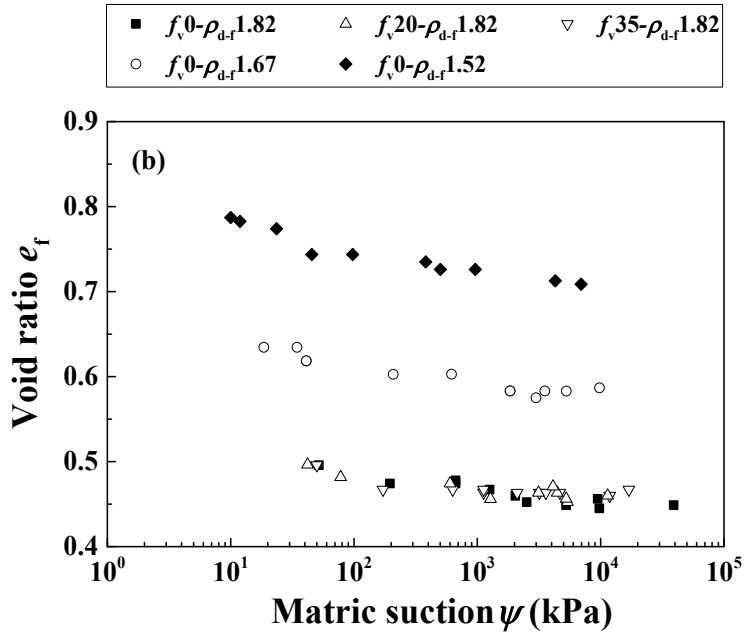

638

639

640

641

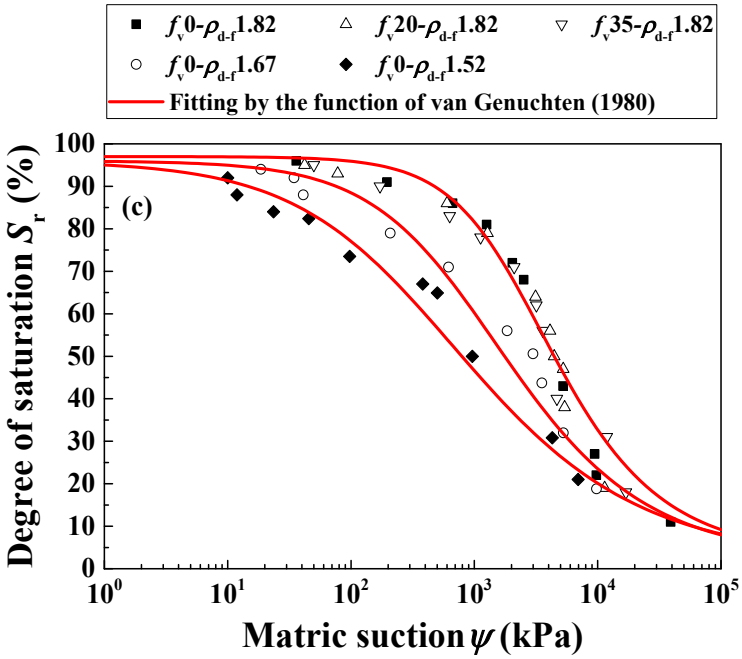

642

643 Fig. 7. Drying soil-water retention curves and variations of void ratios of fine soil with matric
644 suction for varying f_v and $\rho_{d\text{-}f}$ values: (a) gravimetric water content of fine soil versus matric
645 suction; (b) void ratio of fine soil versus matric suction; (c) degree of saturation versus matric
646 suction

647

648

649

650

651

652

653

654

655

656

657

658

659

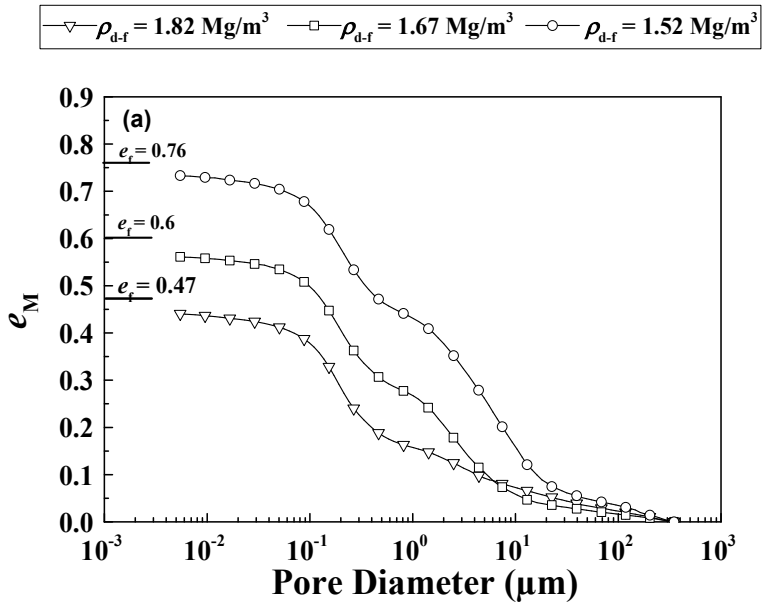

660

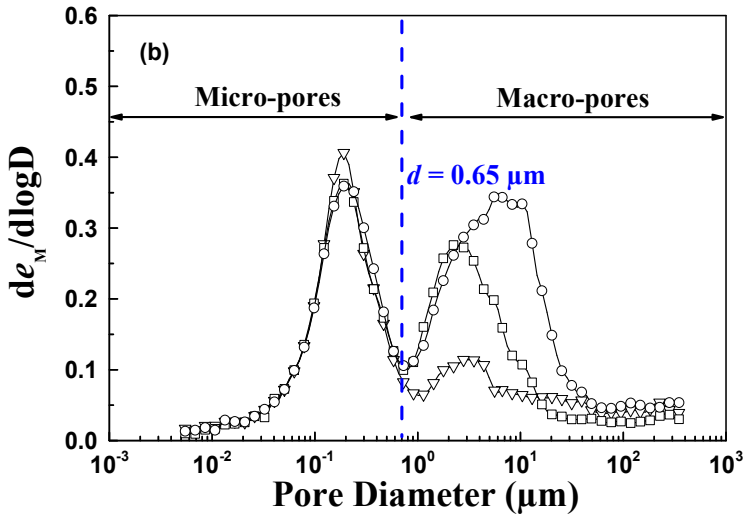

661

662 Fig. 8. Pore size distributions of fine soil at f_v = 0% and different $\rho_{d\text{-}f}$ values: (a) cumulative

663 curves; (b) density function curves

664

665

666

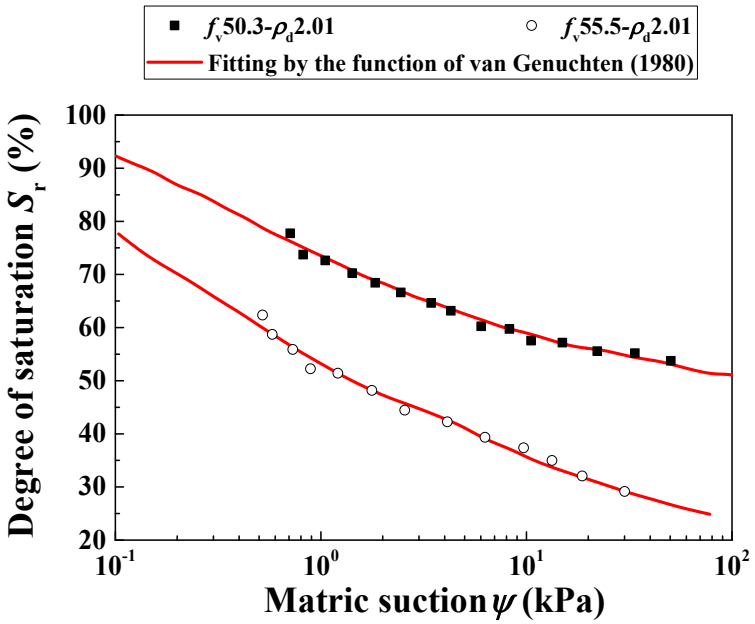

Fig. 9. Drying soil-water retention curves in the study of Duong et al. (2014)

685

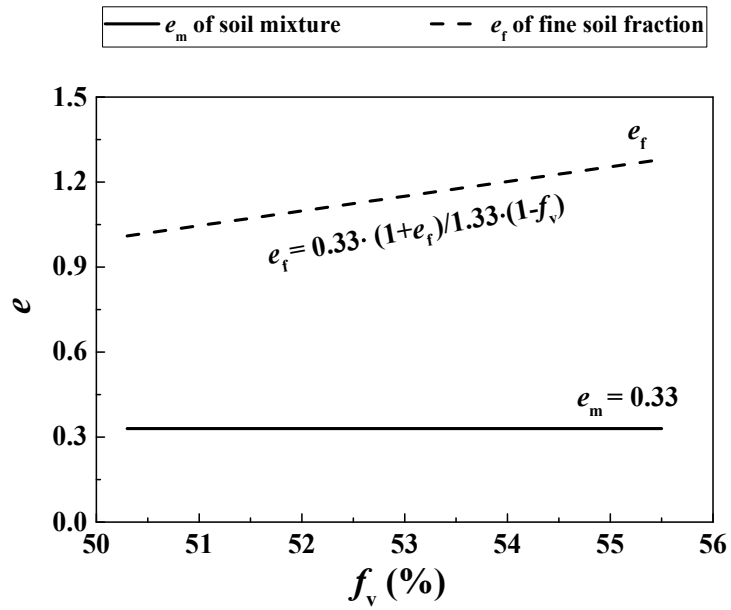

686

687 Fig. 10. Variations of void ratio with f_v at $\rho_d = 2.01$ Mg/m^3 in Duong et al. (2014)

688